

Enhanced emission and light control with tapered plasmonic nanoantennas

Ivan S. Maksymov,^{a)} Arthur R. Davoyan, and Yuri S. Kivshar

Nonlinear Physics Centre, Research School of Physics and Engineering, Australian National University, Canberra ACT 0200, Australia

(Received 17 March 2011; accepted 8 August 2011; published online 23 August 2011)

We introduce a design of Yagi-Uda plasmonic nanoantennas for enhancing the directive gain and achieving control over the angular emission of light. We demonstrate that tapering of nanoantenna elements allows to decrease the inter-element spacing tenfold also enhancing the emission directivity. We find the optimal tapering angle that provides the maximum directivity enhancement and the minimum end-fire beamwidth. © 2011 American Institute of Physics. [doi:10.1063/1.3629787]

Plasmonic nanoantennas are used to couple free-propagating radiation to subwavelength confined regions,^{1,2} enhance and quantize the emission of single quantum emitters such as single molecules or single quantum dots,^{3,4} and offer flexible control over the directionality of nanofocused light.⁵

Recently, rapid progress has been made in the realization of directional control over radiation from single quantum emitters by means of plasmonic Yagi-Uda nanoantennas composed of appropriately arranged metal nanoparticles.^{6–10} High directivity of such plasmonic nanoantennas originates from the uniqueness of their construction inspired from radio frequency (RF) technology. A classical RF Yagi-Uda antenna^{11,12} employs mutual coupling between standing-wave current elements to produce a traveling-wave unidirectional pattern. It uses parasitic elements around an active feed element for reflector and directors to produce an end-fire beam.

In order to fully explore the potential of the communication of energy to, from, and between single quantum emitters, plasmonic Yagi-Uda nanoantennas should have higher antenna gain and offer control mechanisms over the directivity. These aims can be achieved by increasing the length of the nanoantenna along the end-fire beam direction by incrementing the number of directors. While the control over the directionality does not present significant difficulties at RF frequencies, at optical frequencies, absorption losses impose severe restrictions on the length of the nanoantenna. Specifically, the optical response of noble metals such as gold or silver is given by their complex dielectric constants characterized by a negative real part and a positive imaginary part. The latter describes the absorption of radiation energy in the material. Since the electric field of localized surface plasmon modes penetrates into the elements of the nanoantenna, metal absorption losses, which are a function of the electric field intensity and the imaginary part of the dielectric function of the constituent material, increase as the number of directors increases, and the effect from the nanoantenna lengthening comes to naught.

The restriction on the length and consequently the directivity of the plasmonic nanoantenna imposed by the inevitable metal losses in the additional directors can be overcome by slowly tapering the length of the directors. The improve-

ment of the directivity of RF Yagi-Uda antennas by slowly varying the length of directors was suggested by Sengupta¹³ in 1959. But his idea has been abandoned in the modern RF antenna technique because the suggested tapering can be applied to long Yagi-Uda antennas only and results in heavy constructions. At optical frequencies, tapering of the plasmonic waveguides^{14–16} was suggested as an effective tool for nanofocusing of plasmons. The effect of the taper shape and the optimal taper angle on nanofocusing has been discussed actively in the literature (see, e.g., Ref. 17).

In this letter, we suggest an approach for directional control of plasmonic nanoantennas by employing the concept of tapered plasmonic waveguides and a design principle of plasmonic Yagi-Uda nanoantennas for the substantial enhancement of the antenna gain and control of its directivity. We demonstrate that, in contrast to classical design principles, the spacing between the elements of plasmonic nanoantennas can be decreased tenfold and the directivity can be enhanced by slowly tapering the elements length. We obtain numerically the optimal tapering angle that provides the maximum directivity enhancement and the minimum end-fire beamwidth.

For the purpose of demonstration, we consider a two-dimensional model of a 5-element and a 42-element silver plasmonic Yagi-Uda nanoantennas embedded in air and designed according to the effective wavelength rescaling approach¹⁸ relying on a linearly scaled effective wavelength introduced to account for antenna geometry and metal properties at optical frequencies. This rescaling offers additional degrees of freedom in designing nanoantennas with shorter element lengths and inter-element spacings than those used in classical RF antennas.

The schematics of the considered 5-element nanoantenna are shown in Fig. 1(a). The nanoantenna consists of a resonant reflector, the feed of, and equally spaced directors. The length of the feed is $L_f = \lambda_0/4$, where $\lambda_0 = 1550$ nm is the emitted wavelength. The reflector element of length $L_r = 1.25L_f$ is inductively detuned to resonate at wavelengths longer than the resonate wavelength of the feed. The directors of length $L_d = 0.9L_f$ are capacitively detuned to resonate at wavelengths shorter than the resonate wavelength of the feed. The width of all elements is $a = 50$ nm and the spacing between all element is $w = 30$ nm. According to Refs. 6 and 7, the quantum emitter (pointlike, with a vacuum wavelength λ_0) having an in-plane x -polarized dipole is placed near one of the ends

^{a)}Electronic mail: mis124@physics.anu.edu.au.

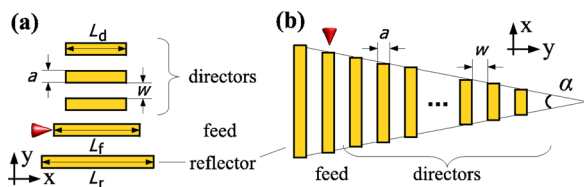


FIG. 1. (Color online) (a) Five-element plasmonic Yagi-Uda nanoantenna. (b) Tapered plasmonic Yagi-Uda nanoantenna. The arrow denotes the position and the polarization of the emitter.

of the feed element. This layout ensures a strong near-field coupling to the feed mode because the position of the emitter coincides with a position of high electric mode density.¹⁹

The angular dependence of the emission of both nanoantennas is studied first. We use the finite-element method (FEM, COMSOL MULTIPHYSICS 4.0) and consider the electromagnetic fields lying in the XY -plane (Fig. 1). The dielectric function of silver used in the simulations is based on a Drude model fit for the published optical constants of silver.²⁰ According to Ref. 11, the performance of the investigated nanoantennas is discussed in terms of the angular directivity defined as $D(\theta) = \frac{2\pi P(\theta)}{P_{\text{loss}} + P_{\text{rad}}}$, where $P(\theta)$ is the angular radiated power, P_{rad} is the Poynting vector flux through a closed contour in the far-field region, and P_{loss} is the absorption losses.

Figure 2(a) shows the emission pattern of the 5-element and 42-element nanoantennas. It demonstrates that the 5-element antenna with the spacings between the elements of just 30 nm offers a typical directivity as compared to a similar nanoantenna designed according to the classical design principles.⁷ Simulations for the 42-element nanoantenna with the same element dimensions and inter-element spacings but with an increased number of directors demonstrate that the increase in the total length of the nanoantenna does not change the directivity and just slightly decreases the width of the main lobe. Indeed, as shown in Fig. 2(a), the maximum emission directivity [defined as $D_{\text{max}} = \max(D(\theta))$] for the 42-element nanoantenna equals to that of the 5-element nanoantenna. The analysis of the near-field profiles of the generated end-fire beams [Figs. 2(b) and 2(c)] convincingly confirms a poor performance of the elongated nanoantenna. This result contradicts the predictions of the classical antenna theory¹² because the benefit from the augmentation of the number of directors is brought to naught by absorption losses in the metallic elements.

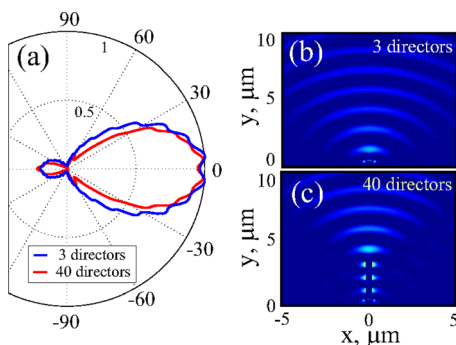


FIG. 2. (Color online) (a) Angular emission patterns of the 5-element and 42-element Yagi-Uda nanoantennas. (b) and (c) Real part of E_x electric fields of the 5-element and 42-element Yagi-Uda nanoantennas.

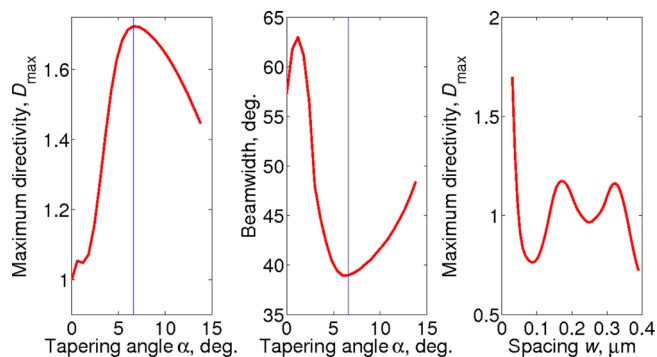


FIG. 3. (Color online) (a) Maximum emission directivity D_{max} and (b) beamwidth of the tapered 42-element Yagi-Uda nanoantenna as a function of α . The straight lines highlight $\alpha_{\text{opt}} = 6.6^\circ$. (c) D_{max} at $\alpha_{\text{opt}} = 6.6^\circ$ as a function of the spacing w .

Now, we turn our attention to the tapered antenna [Fig. 1(b)]. The length of the feed and the length of the reflector of the tapered nanoantenna, the width of all elements, and the spacings between them equal to the corresponding dimensions of the nanoantennas without the tapering [Fig. 1(a)]. The length of the directors is slowly tapered as a function of the tapering angle α according to the formula $L(x) = L_f - 2(W + a)tg(\alpha)$, where L_f is the feed length, a is the width of the directors, and $W = Nw$ is the spatial coordinate of the center of the N th director.

Fig. 3(a) plots the maximum emission directivity D_{max} normalized to the maximum directivity of the 42-element nanoantenna without tapering as a function of the tapering angle α . The beamwidth, defined as the angular separation between two identical points on opposite side of the pattern half-maximum,¹¹ is plotted in Fig. 3(b) also as a function of α . A pronounced maximum of the directivity [Fig. 3(a)] and a minimum of the beamwidth [Fig. 3(b)] are observed at $\alpha_{\text{opt}} = 6.6^\circ$, which is hereafter referred to as the optimal tapering angle.

In contrast to the nanoantenna without tapering ($\alpha = 0$), the optimally tapered antenna offers a more than one-and-a-half superior directivity accompanied by a $\sim 20^\circ$ decrease in the beamwidth, which is a considerable advantage that originates from the effect of the optimal tapering¹⁷ accompanied by a decrease in absorption losses due to the reduction of the metallic elements. Despite a further decrease in absorption offered by the nanoantenna with $\alpha = 12.2^\circ$, its directivity deteriorates as compared to the nanoantenna with the optimal tapering angle (however, the directivity at $\alpha = 12.2^\circ$ is still superior than that of the nanoantenna without tapering).

In order to demonstrate the impact of the tapering on the directivity, we repeat the calculations of the angular emission patterns and the near-field distributions for three different 42-element Yagi-Uda nanoantennas without tapering ($\alpha = 0$), with the optimal tapering angle ($\alpha_{\text{opt}} = 6.6^\circ$), and with a higher than optimal tapering angle ($\alpha = 12.2^\circ$), respectively. The calculated emission patterns are shown in Fig. 4(a). According to the result in Fig. 3, in Fig. 4(a), we observe a ~ 1.7 increase in the maximum directivity and a substantial narrowing of the end-fire beam. A broadened beam pattern confirms the prediction of Fig. 3 at $\alpha > \alpha_{\text{opt}}$.

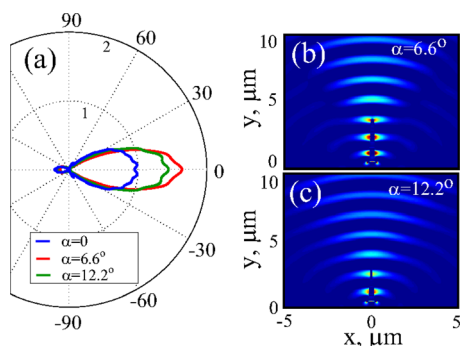


FIG. 4. (Color online) (a) Angular emission patterns of 42-element Yagi-Uda nanoantennas without tapering ($\alpha=0$), with the optimal tapering ($\alpha_{opt}=6.6^\circ$), and with a non-optimized tapering ($\alpha=12.2^\circ$). (b) and (c) Real part of E_x electric fields of the antenna with $\alpha_{opt}=6.6^\circ$ and $\alpha=12.2^\circ$. The same scale as in Figs. 2(b) and 2(c) is used.

The calculated near-field profiles [Figs. 4(b) and 4(c)] reveal that at the optimal tapering angle, the field propagates to the tapered end of the nanoantenna and a narrow end-fire beam is formed. In contrast, at tapering angles $\alpha > \alpha_{opt}$, the field is not confined to the directors and jumps off before it reaches the end of the nanoantenna.

These results convincingly confirm that the tapering with the optimal angle allows enhancing the directivity of the 42-element plasmonic Yagi-Uda nanoantenna. We remind that this result is achieved with a 30 nm spacing between the nanoantenna elements, which equals to just one tenth of the spacing of state-of-the-art plasmonic Yagi-Uda nanoantennas.^{6,8}

The elements of the nanoantenna with α_{opt} , including the smallest director of 50×250 nm and spacings of 30 nm, can be fabricated using current fabrication technologies.² In Fig. 3(c), we plot D_{max} as a function of the spacing w ($w < 20$ nm are hardly attainable in practice and not considered). It reveals a low sensitivity of D_{max} to changes in the spacing by ± 10 nm. It also shows that the tapering offers advantages even with larger spacings.

More importantly, the suggested nanoantenna is also stable to fabrication errors in the length of the directors. Owing to a narrow spacing, the fundamental mode of the tapered nanoantenna propagates on the outer boundary of the directors and thus should be tolerant to changes in the length of the directors. This assumption is convincingly supported by

statistical simulations using a normal distribution random number generator. We take average of D_{max} at λ_0 over 100 independent realizations and show that random changes in the length of the directors by ± 5 nm decrease D_{max} by $\sim 7\%$ as compared with the defectless nanoantenna. We notice that the considered error range of ± 5 nm is greater than the length difference of 3 nm between adjacent directors.

In conclusion, we have applied the concept of tapered plasmonic waveguides to plasmonic Yagi-Uda nanoantennas and suggested the enhanced emission directivity and reduction of the total nanoantenna length. We expect that a small footprint of the proposed nanoantennas will make them attractive for application to horizontal on-chip plasmonic wireless signal-transmission circuits.

The authors thank Andrey Miroshnichenko for valuable discussions. This work was supported by the Australian Research Council.

- ¹P. Bharadwaj, B. Deutsch, and L. Novotny, *Adv. Opt. Photon.* **1**, 438 (2009).
- ²L. Novotny and N. F. van Hulst, *Nature Photon.* **5**, 83 (2011).
- ³A. Huck, S. Kumar, A. Shakoor, and U. K. Andersen, *Phys. Rev. Lett.* **106**, 096801 (2011).
- ⁴I. S. Maksymov, M. Besbes, J. P. Hugonin, J. Yang, A. Beveratos, I. Sagnes, I. Robert-Philip, and P. Lalanne, *Phys. Rev. Lett.* **105**, 180502 (2010).
- ⁵T. Shegai, V. D. Miljković, K. Bao, H. Xu, P. Nordlander, P. Johansson, and M. Käll, *Nano. Lett.* **11**, 706 (2011).
- ⁶A. G. Curto, G. Volpe, T. H. Taminiau, M. P. Kreuzer, R. Quidant, and N. F. van Hulst, *Science* **329**, 930 (2010).
- ⁷T. H. Taminiau, F. D. Stefani, and N. F. van Hulst, *Opt. Express* **6**, 16858 (2008).
- ⁸T. Kosako, Y. Kadoya, and H. F. Hofmann, *Nature. Photon.* **4**, 312 (2010).
- ⁹H. F. Hofmann, T. Kosako, and Y. Kadoya, *New J. Phys.* **9**, 217 (2007).
- ¹⁰A. F. Koenderink, *Nano Lett.* **9**, 4228 (2009).
- ¹¹C. A. Balanis, *Antenna Theory: Analysis and Design* (John Wiley and Sons, New Jersey, 2005).
- ¹²T. A. Milligan, *Modern Antenna Design* (John Wiley and Sons, New Jersey, 2005).
- ¹³D. L. Sengupta, *IRE Trans. Antennas Propag.* **8**, 11 (1960).
- ¹⁴K. V. Nerkaryan, *Phys. Lett. A* **237**, 103 (1997).
- ¹⁵M. I. Stockman, *Phys. Rev. Lett.* **93**, 137404 (2004).
- ¹⁶A. R. Davoyan, I. V. Shadrivov, A. A. Zharov, D. K. Gramotnev, and Yu. S. Kivshar, *Phys. Rev. Lett.* **105**, 116804 (2010).
- ¹⁷A. R. Davoyan, I. V. Shadrivov, Yu. S. Kivshar, and D. K. Gramotnev, *Phys. Status Solidi (RRL)* **4**, 277 (2010).
- ¹⁸L. Novotny, *Phys. Rev. Lett.* **98**, 266802 (2007).
- ¹⁹D. E. Chang, A. O. Sørensen, P. R. Hemmer, and M. D. Lukin, *Phys. Rev. Lett.* **97**, 053002 (2006).
- ²⁰E. D. Palik, *Handbook of Optical Constants of Solids* (Academic, New York, 1985).